Journal of Theoretical and Applied Physics
a SpringerOpen Journal

RESEARCH Open Access

Thermoelectric power of metallic Rb_3C_{60}: phonon-drag and carrier diffusion contributions

Dinesh Varshney[1*] and Namita Singh[2]

Abstract

Thermoelectric power (S) of Rb_3C_{60} fullerides in the metallic phase is theoretically estimated. We first develop a Hamiltonian model that incorporates the scattering rates within the relaxation time approximation to estimate the phonon-drag thermoelectric power (S_{ph}^{drag}) incorporating the scattering of phonons with defects, electrons as carriers, grain boundaries, and phonon-phonon interactions. As a next step, Mott expression within parabolic band approximation is used to analyze the electron diffusive thermoelectric power (S_c^{diff}) using Fermi energy as electron parameter, and S_c^{diff} shows a linear temperature dependence. The S_{ph}^{drag} is nonzero in both normal and superconducting states. Its behavior is determined by competition among the several operating scattering rates for heat carriers and a balance between diffusive carrier and phonon-drag contributions. Acoustic phonons are effectively scattered by various scatterers for the thermoelectric power. S infers a change in slope above transition temperature and becomes almost linear above 70 K.

Keywords: Rb_3C_{60}, Thermoelectric power, Phonon drag, Carrier diffusion, Intermolecular phonon

Background

Since the revolution of superconductivity in organic materials, initiated by Hebard and researchers [1], the unusual normal state transport properties of alkali-metal-intercalated fullerides have been suspected of giving clues to the basic mechanism responsible for superconductivity [2,3]. The parent C_{60} is a typical insulator, and by doping with alkali-metal atoms, M_3C_{60} (which opt for a face-centered cubic structure) superconductivity in intercalated compounds will appear in limited conditions. Prominent among these materials are the M_3C_{60} fullerides with M standing for K, Rb, or Cs with a superconducting transition temperature T_c of approximately 40 K (Rb_3C_{60}) at ambient pressure. Alkali-metal-intercalated C_{60} continues to generate excitement due to the conducting polymeric phase in MC_{60} [4]. It is identified that in alkali-metal-doped fullerenes, the phonon spectrum has a wide frequency region. The vibrational spectrum is classified into two regions. One of them belongs to the rotation of C_{60} molecule and the intermolecular vibrations. The others belong to the intramolecular vibrations. Actually, the intramolecular phonons span a large frequency range, from 2×10^2 to 2×10^3 cm^{-1}, while intermolecular vibrations and soccer ball vibrations (restricted rotations) go down to a low energy interval, 10 to 100 cm^{-1} [5]. The electronic structure of alkali-metal-doped fullerenes in the normal state is important in understanding the mechanism of superconductivity. Switching to electronic structure, experimental techniques as NMR measurements [6], photoemission measurements [7], and infrared reflectivity measurements [8] report the bandwidth ranging from 0.2 to 1.2 eV.

It is identified that in alkali-metal-doped fullerenes, the phonon spectrum has a wide frequency region. The vibrational spectrum is classified into two regions. One of them belongs to the rotation of C_{60} molecule and the intermolecular vibrations. The others are the intramolecular vibrations. Actually, the intramolecular phonons span a large frequency range, $2 \times 10^2 - 2 \times 10^3$ cm^{-1}, while intermolecular vibrations and soccer ball vibrations (restricted rotations) go down to a low energy interval, 10 – 100 cm^{-1} [5]. The electronic structure of alkali-metal-doped fullerenes in the normal state is important for understanding the mechanism of superconductivity. Switching to electronic structure, experimental techniques as NMR measurements [6], photoemission

* Correspondence: vdinesh33@rediffmail.com
[1]Materials Science Laboratory, School of Physics, Vigyan Bhawan, Devi Ahilya University, Khandwa Road Campus, Indore 452001, India
Full list of author information is available at the end of the article

measurements [7] and infrared reflectivity measurements [8] reports the bandwidth ranging from 0.2 to 1.2 eV.

Doping of alkali metal in the parent C_{60} essentially expands the lattice and causes an increase in the lattice constant; the result is the enhanced density of states at the Fermi level $N(\varepsilon_F)$. An intermediate consequence is a fairly large electron-phonon interaction ($\lambda \equiv N(\varepsilon_F)V$)) depending upon whether inter- or intramolecular phonon is the mediating boson. The thermoelectric power $S(T)$ is a powerful probe not only to understand the electronic structure, but also to shed light on the electron-phonon interaction. The mass enhancement effects can increase the thermoelectric power of a metal at low temperatures [9]. The mass enhancement is proportional to $(1 + \lambda)$, and this correction is normally masked by large phonon-drag effect.

In contrast to conventional superconductors, the physical properties of organic superconductors directly reflect the electronic structure of the molecules they consist. Inabe et al. have first reported the thermoelectric power of single crystal K_3C_{60} and Rb_3C_{60} superconductors [10]. Nonlinear temperature dependences of $S(T)$ with negative sign are documented above T_c for both K- and Rb-doped fullerides. The room-temperature value of $S(T)$ is about −11 μV/K, indicating the metallic nature in the normal state with electron as sole carriers. The absolute value of S decreases linearly until it drops discontinuously to zero at T_c and at a broad hump around 70 K. The analysis of density of states in K_3C_{60} reveals that low-frequency phonon modes are significant in normal state transport, and the nonlinear behavior in low-temperature regime ($T < 70$ K) is ascribed to phonon drag.

The measured thermoelectric power in K_4C_{70} thin films also shows a negative S, indicating that charge carriers are electrons and that roughly linear temperature dependence is below 100 K. For higher temperatures $T > 100$ K, $S(T)$ decreases slowly with a deviation from linearity [11]. Since the conduction band in K_4C_{70} is half-filled, similar to that of K_3C_{60}, an estimate of bandwidth is about 0.5 to 0.6 eV, consistent with a value of approximately 0.6 eV in K_3C_{60}. Henceforth, the normal state of K_3C_{60} is a metallic state with a bandwidth of approximately 0.6 eV; the electron-phonon interaction and electron-electron interaction are important for charge transport.

Later on, Suighara et al. have discussed the possibility of phonon-drag thermopower in doped fullerides [12]. It is concluded that a small but clear deviation from the linear relation at low temperatures is ascribed to the phonon-drag effect. The broad dip over 100 K and its small magnitude suggest that the anomaly is not related to the electron-intramolecular phonon interaction but to the electron-intermolecular phonon interaction. A visual comparison of data indicates that the temperature dependence of the thermopower of superconducting fullerenes is very similar to that of systems in which mass enhancement effect has been observable [13,14].

Motivated by the available experimental data [10-12] and carrier diffusion term with mass enhancement [13], for thermoelectric power, we plan to seek the role of scattering of phonon with defects, grain boundaries, phonon and electrons for phonon-drag thermoelectric power, as well as the carrier diffusion contribution. This improves our understanding of the interplay of scattering processes between heat carriers themselves and between carriers and impurities for the explanation of the reported behavior of thermoelectric power $S(T)$. Also, it is important to look for the relative magnitudes of these scattering processes, which lead to the anomalous behavior, and this is another motivation for the present investigation. The results we report here indeed shed some very important light on the nature of phonon and electron as carrier channel of thermoelectric power in Rb_3C_{60}.

We first describe the method of calculation, give further details of the results, and speculate on the reliability of our approach to the problem of $S(T)$ in alkali-metal-doped fullerides. In 'The model' section, we give details about the scattering rates within the relaxation time approximation to estimate the phonon-drag thermoelectric power ($S_{\mathrm{ph}}^{\mathrm{drag}}$) incorporating the scattering of phonons with defects, electrons as carriers, grain boundaries, and phonon-phonon interactions. While obtaining numerical results, we place particular emphasis on the acoustic phonons as a source of $S_{\mathrm{ph}}^{\mathrm{drag}}$ in the Hamiltonian model. Also, the role of carrier diffusion contribution up to room temperature and zero magnetic field for $S(T)$ is investigated. We find that the $S(T)$ behavior can be well accounted for through the use of the Debye model. In the 'Results and discussion' section, we give the numerical estimation of various scattering rates for the calculation of diffusion and phonon-drag processes and discuss the results obtained. In the 'Conclusions' section, we provide physical descriptions of the numerical results calculated herein.

The model

Let us begin with the estimation of carrier diffusion thermoelectric power. We use the well-known Mott formula within parabolic band approximation to estimate the contribution of electrons towards thermoelectric power. The low-temperature carrier diffusion thermoelectric power [10] is as follows

$$S_{\mathrm{c}}^{\mathrm{diff.}}(T) = -\frac{\pi^2 k_B^2 T}{3|e|}\left[\frac{\partial \ln \sigma(\varepsilon)}{\partial \varepsilon}\right]_{\varepsilon=\varepsilon_F}. \quad (1)$$

with $\sigma(\omega) = ne^2\tau(\varepsilon)/m$ as the energy dependence of electrical conductivity in the relaxation time approximation.

Here, $n(m)$ is the density (mass) of carriers, and τ is the relaxation time. Moreover, this expression is true within parabolic band approximation, but not with relaxation time approximation alone. For the sake of simplicity, it is sufficient to neglect the energy dependence in τ (ε), taking τ (ε) = τ (ε_F); for three-dimensional model, Equation 1 becomes the following

$$S_{\mathrm{c}}^{\mathrm{diff.}}(T) = -\frac{\pi^2 k_B^2 T}{6|e|\varepsilon_F}. \tag{2}$$

Keeping in mind that $\tau = \ell/v_F$, the method point to the scattering of carriers by impurities is dominant for constant relaxation times. Such a procedure has found success in explaining previous measurements on high-temperature superconductors on a wide temperature range [15,16].

As a next step, in order to assess the role of phonons for thermoelectric power, we develop a Hamiltonian model where the low-energy intermolecular vibrations (phonons) in Rb_3C_{60} are described in the Debye model, and the electrons as charge carriers are treated in an isotropic Bardeen-Cooper-Schrieffer (BCS)-like model. The charge carriers are quasiparticles in a periodic crystal and hence have a well-defined dispersion relation ε_k. The alkali-metal-doped fullerides are impure crystals, where the excitations may not be quasiparticles at all, but for which the physical properties are qualitatively same.

The phonon inelastic scattering events are assumed to be independent, and scattering of phonon with various scattering sources is additive. The Debye model with acoustic phonon is valid for Rb_3C_{60} as the temperature domain of interest lies well below the effective Debye temperature $\theta_D \approx 185$ K [17]. We shall use the isotropic BCS-like model with intermolecular acoustic phonon to derive qualitative results for thermoelectric power.

The Hamiltonian model is as follows [18]:

$$\begin{aligned} H = &\sum_p \varepsilon_p a_p^+ a_p + \sum_q \omega_q b_q^+ b_q + \sum_{p_1,p_2} \phi(p_1,p_2) a_{p_1}^+ a_{p_2} \\ &+ D_p \sum_{p,q} q \left[\frac{\hbar}{2\rho\omega_q}\right]^{1/2} a_{p+q}^+ a_p \left(b_p + b_{-q}^+\right) \\ &+ \frac{R}{2n} \sum_{q_1,q_2} e^{i(q_1+q_2)R_i} \left[\frac{\hbar\omega_{q_1}\hbar\omega_{q_2}}{4}\right]^{1/2} \left(b_{q_1} - b_{-q_1}^+\right) \\ &\times \left(b_{q_2} - b_{-q_2}^+\right) + H_{p-p}. \end{aligned} \tag{3}$$

The initial two terms are carrier (electron) and phonon excitations; the third and fourth terms represent carrier-impurity and carrier-phonon interactions, respectively. The fifth term is phonon-impurity interaction, and the last term stands for the phonon-phonon interaction. The symbols that appeared in Equation 3 are as follows: ε_p is the carrier free energy, a (a^+) and b (b^+) are the creation (annihilation) operators for phonon and electron, $\underline{\phi}$ is coupling parameter of electron and impurity potential, D_p is deformation-potential constant, ρ is ionic mass density, ω_q is acoustic phonon frequency of a wave vector **q**, R is relative ionic-mass difference ((M'' – M) / M''), M (M'') symbolizes for C_{60} (Rb), n is number of cells, and R_i stands for the position of defects due to substitutions.

To estimate the phonon-drag thermoelectric power, we shall use the Kubo formula following the Hamiltonian model [19]. It has contributions from both the phonons and the carriers. In the continuum approximation, the lattice part is as follows [20]:

$$S_{\mathrm{ph}}^{\mathrm{drag}}(T) = -\frac{k_B}{|e|}\left[\frac{T}{\theta_D}\right]^3 \int_0^{\omega_D} d\omega(\beta\omega)^4 A(\omega)(\beta\omega)^4 \frac{e^{\beta\omega}}{\left(e^{\beta\omega}-1\right)^2}. \tag{4}$$

The Boltzman constant is k_B; e is the charge of carriers, ω_D is the Debye frequency, and $\beta = \hbar/k_BT$.

The relaxation time is inhibited in $A(\omega)$ and is proportional to the imaginary part of the self-energy Σ. The relaxation time ratio can be calculated to the lowest order of the various interactions in the weak interaction case. The phonon-drag thermoelectric power relaxation time ratio A (ω) is as follows:

$$\begin{aligned} A(\omega) = &\left[1/\tau_{ph-d} + 1/\tau_{ph-gb} + 1/\tau_{ph-ph}\right]^{-1} \\ &\times \left[1/\tau_{ph-d} + 1/\tau_{ph-gb} + 1/\tau_{ph-ph} + 1/\tau_{ph-c}\right], \end{aligned} \tag{5}$$

The relaxation times are expressed as follows:

$$\tau_{ph-d}^{-1}(\omega) = D_{phd}/k_B^3\omega^4\hbar^3. \tag{6}$$

The various relaxation times are defined in terms of transport coefficients as in the following:

$$\tau_{ph-d}^{-1}(\omega) = D_{phd}/k_B^3\omega^4\hbar^3, \tag{7}$$

$$\tau_{ph-gb}^{-1}(\omega) = D_{phgb}v_s/L, \tag{8}$$

$$\tau_{ph-ph}^{-1}(\omega) = D_{phph}(T\omega\hbar/k_B)^3, \tag{9}$$

and

$$\tau_{ph-c}^{-1}(\omega) = D_{phe}\omega n_F(\Delta), \tag{10}$$

where v_s is the velocity of sound, L is the crystal dimension, n_F is the Fermi-Dirac distribution function, and Δ is the energy gap parameter. The notations $\tau_{ph\text{-}d}$, $\tau_{ph\text{-}gb}$, $\tau_{ph\text{-}ph}$, and $\tau_{ph\text{-}c}$ are the phonon scattering relaxation time due to substitutional defects, grain boundaries, phonon-phonon interaction, and phonon-carrier interaction, respectively. We note that to this order, Mathiessen's rule holds: the inverse of the total relaxation time is the

sum of the various contributions for the different scattering channels.

The transport coefficients appearing in Equations 7 to 10 are defined as

$$D_{\text{phd}} = \left[\frac{3n_i R^2}{4\theta_D^3}\right], \tag{11}$$

with n_i as the density of impurities or point defects, R is the relative ionic-mass difference, and θ_D the Debye temperature. The above essentially accounts for the density of real point defects in Rb_3C_{60}, such as impurities, vacancies, and interstitials, which should be fairly large in a weakly bound crystal such as orientationally ordered C_{60} and increase in orientationally disordered Rb_3C_{60}. The potential exerted on electron as free carriers in the doped C_{60} is due to the ionized cage of orientationally ordered C_{60}. The strength of the electron-phonon scattering in terms of deformation potential D_p, carrier mass m, ionic mass M, and the Fermi energy (ε_F) is as follows:

$$D_{\text{phe}} = \frac{9\pi}{4}\left[\frac{m}{3M}\right]^{1/2}\frac{{D_p}^2}{\varepsilon_F^2}, \tag{12}$$

Herein, the Thomas-Fermi approximation defines the electron-acoustic phonon coupling strength as $D_p = -\varepsilon_F / 2$.

The estimation and numerical computation of the carrier diffusion and phonon-drag contributions to the thermoelectric power by incorporating the effects of different scattering mechanisms are presented in the 'Results and discussion' section.

Results and discussion

We first estimate the carrier diffusion thermoelectric power (S_c^{diff}), which is given by the expressions (Equations 1 and 2). The Fermi energy ε_F in Rb_3C_{60} is calculated as 0.23 eV, which is used for the computation of S_c^{diff}. The carrier-impurity contribution to the thermoelectric power S_c^{diff} is documented in Figure 1 as functions of temperature. It is evident from the plot that $S_c^{\text{diff}}(T)$ increases linearly with increasing temperature. The numerically computed S_c^{diff} is subtracted from the experimental data [10] to obtain the difference ($S_{\text{difference}} = S_{\text{experimental}} - S_c^{\text{diff}}$). The difference $S_{\text{difference}}$ is characterized as phonon-drag thermoelectric power and fitted within the relaxation time approximation.

The thermoelectric power is a powerful probe to study the nature of carriers and scattering process between them in the phonon system with either the absence or presence of a magnetic field. For the actual calculation of the phonon-drag thermoelectric power in Rb_3C_{60}, more realistic values of some physical parameters derived from the experimental data follows. The Coulomb interactions among the adjacent ions in an ionic crystal such as Rb_3C_{60} are expressed in terms of inverse-power overlap repulsion as in the following [21]:

$$\Phi(r) = -(Ze)^2\left[\frac{1}{r} - \frac{f}{r^s}\right], \tag{13}$$

with f is being the repulsion force parameter between the ion cores.

The elastic force constant $\underline{\kappa}$ is conveniently derived from $\Phi(r)$ at the equilibrium interionic distance r_0 as of the following:

$$\begin{aligned}\kappa &= \left(\frac{\partial^2\Phi}{\partial r^2}\right)_{r_0},\\ &= (Ze)^2\left[\frac{s-1}{r_0^3}\right],\end{aligned} \tag{14}$$

Here, s is the index number of the overlap repulsive potential. For Rb_3C_{60}, the acoustic mass M = (M (Rb) + M (C_{60})) is 979.29 amu. The elastic force constant $\kappa^* = 2\kappa$ for each directional oscillation mode to get the acoustic phonon frequency as follows:

$$\begin{aligned}\omega_D &= \sqrt{\frac{\kappa^*}{2M}},\\ &= (Ze)\sqrt{\frac{(s-1)}{2M}\frac{1}{r_0^3}}.\end{aligned} \tag{15}$$

The acoustic phonon mode frequency is estimated following the ionic model. Here, we have used the value of effective ion charge $Ze = 7e$. The Debye temperature for Rb_3C_{60} is obtained by taking $s = 7$ and the bond distance $r_0 = 10.21$ Å ($a/\sqrt{2}$) ($a = 14.45$ Å) [1], yielding $\kappa = 6.36 \times 10^4$ gm s^{-2}. For most ionic crystals, the index number of the repulsive potential has been reported to be $s = 6$ to 8 [21]. Such procedure yields the Debye temperature of about 95 K.

Deduced value of the Debye temperature is consistent with specific heat data [18], inelastic neutron scattering results [5], isotope effect studies [22], and thermoelectric power data [10,12]. We do not claim the process to be rigorous, but a consistent agreement following spring ball lattice model with repulsive force between Rb cations and C_{60} is obtained to evaluate acoustic phonon energy. We note that the present model has only one free parameter, i.e., the index number of the repulsive potential. Value of θ_D differs from technique to technique, and its value also vary from sample to sample with an average value and standard deviation of $\theta_D = \theta_D \pm 15$ K.

In Rb_3C_{60}, the electron density $n = (4 \times 3/a^3)$ is calculated from the lattice parameter a of 14.45 Å [1] to get $n = 3.98 \times 10^{21}$ cm^{-3}. We have used the band

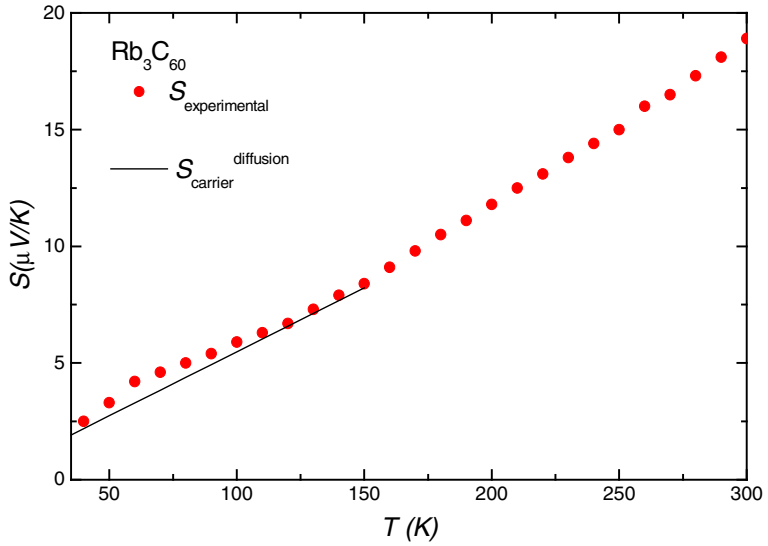

Figure 1 Variation of carrier diffusion thermoelectric power with temperature compared with experimental data. Adapted from Inabe et al. [10] for Rb_3C_{60} superconductors.

structure value of mass as 3.6 m_e [9,20]. The electron parameters such as Fermi velocity and Fermi wave vector are obtained as 1.55 × 10^7 cm s^{-1} and 0.486 $Å^{-1}$, respectively. The length of the sample is about 3 mm and v_s = 2.2 × 10^5 cm s^{-1}. The above corresponds to the weak intermolecular interaction. Herein, we presume that Rb_3C_{60} contains the defects, the phonons, and the BCS-like quasiparticles, interacting with one another as evident from the Hamiltonian model.

While estimating the temperature-dependent thermoelectric power of Rb_3C_{60}, we make use of the transport parameters which characterize the strengths of the phonon defects, phonon-grain boundary, phonon-phonon, and phonon-carrier scattering processes as D_{phd} = 3.1 × 10^{-9} K^{-3}, D_{phgb} = 2.5 × 10^{-2} K^{-6} s^{-1}, D_{phph} = 2.3 × 10^{-3} K^{-6} s^{-1}, and D_{phe} = 5.3 K^{-6} s^{-1}, respectively. These are material-dependent fitting parameters for phonon-drag thermoelectric power in the present model. It is instructive to mention that the electron-phonon interaction is limited to the coupling of intermolecular acoustic phonons. The phonon-drag term is not related to the intramolecular phonons because of an unusual high energy but is responsible for superconductivity in alkali-intercalated fullerides.

We first discuss the relative magnitudes of the various scattering mechanisms. A plot of various scattering phonon relaxation time as a function of ξ ($\xi = \hbar\omega / k_B T$) in terms of frequency at T = 10, and 35 K from Equations 7 to 10 are shown in Figure 2. It can be seen that for low values of ξ, the phonon-electron scattering is higher, while for high values of ξ, it is the phonon-defect scattering that grows faster. However, at both small and large values of ξ, the phonon-phonon scattering process is weaker. As we go above T_c, i.e., with increase in temperature (see Figure 3 in the normal state at T = 50, 150, and 250 K), phonon-electron scattering improves and phonon-phonon scattering becomes weaker. In the superconducting state $T < T_c$, carriers are condensed in Cooper pair; the increase in temperature order parameter reduces the state, and concentration of free carriers increases the state. In particular, phonon-phonon umklapp scattering grows faster than phonon-electron scattering due to a large mobility of carriers in the normal state ($T > T_c$). In this respect, for all temperatures above T_c, the phonon-impurity scattering saturates for higher ξ values.

We now qualitatively discuss S_{ph}^{drag} in the presence of various scattering mechanisms (please see Figure 4). At low temperatures through T_c, the quasiparticle excitations condensed into the ground state, and they did not scatter the phonons. S_{ph}^{drag}, thus, increases exponentially with temperature in the vicinity of transition temperature, As various scatterings of phonons contribute to the reduction of thermal conductivity, it leads to the increase of thermoelectric power. The individual effect on thermoelectric power due to different scattering mechanisms is shown in Figure 4. The results show that the effect of scatterings on thermoelectric power is additive, and the final variation depends on the relative magnitude of different scattering processes available. It is worth to mention that S in the superconducting state is zero ($T \rightarrow 0$ K) and that every nonzero value is an artifact due to the model.

To ascertain the physical significance of the density of impurities, we evaluate the transport coefficient D_{phd} that appeared in Equation 7. We estimate the product of

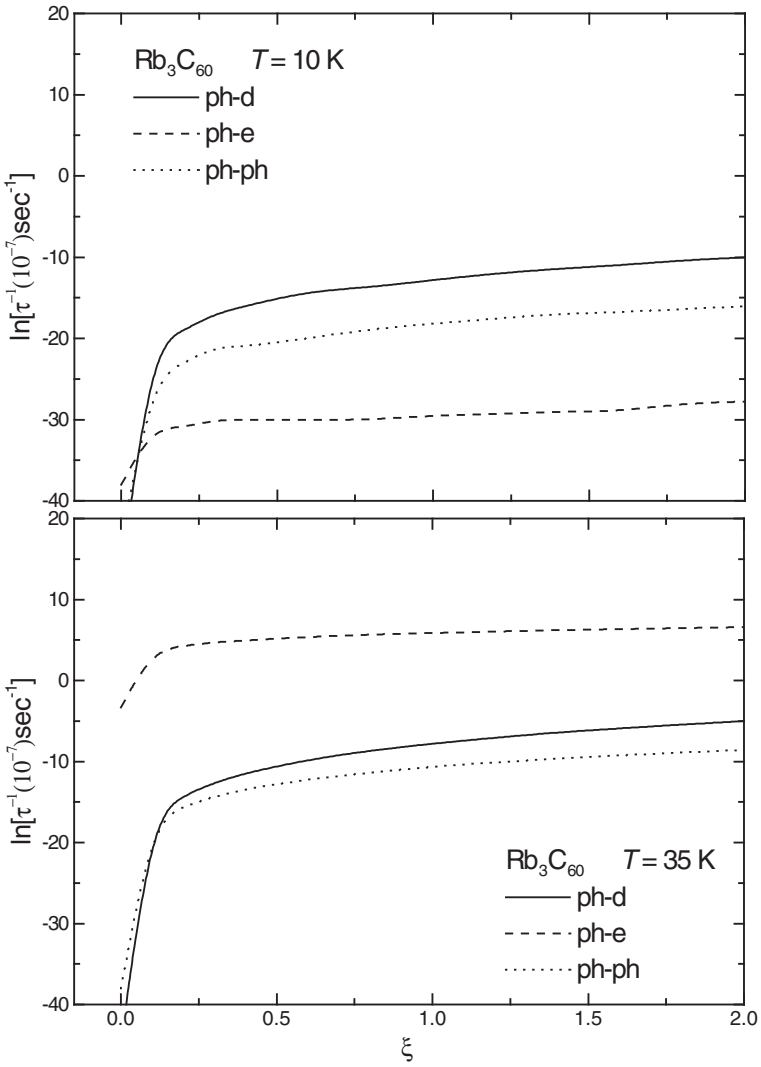

Figure 2 Variation of phonon relaxation times as function of ξ for T = 10 and 35 K. For Rb_3C_{60} superconductors.

density of impurities and square of relative ionic mass difference, $n_i R^2 = 4.91 \times 10^{-3}$, from the value of coefficient D_{phd}. Due to the fact that the transport parameter D_{phd} is determined by the magnitude of the phonon-impurity interaction, we are able to roughly estimate the density of impurity scatterers which may point to the fact that the quasiparticles in the metallic state are essentially localized. In this way, one can set a limit to the concentration of impurities if the impurities as scatterers are isotope in origin. Herein, we believe that the density of impurity is constant with respect to temperature. In passing, we refer to the work of Erwin and Pickett [23] who worked out the lowest-order variational solution for S (T). The energy dependence of scattering rate $1/\tau$ is considered (1) the electron-phonon coupling strength $\lambda(\varepsilon)$ = constant, leading to a free-hole-like thermoelectric power with positive slope and linear behavior and (2) $\lambda(\varepsilon) = N(\varepsilon)$, resulting in an electron behavior up to ≈200 K and a slow transition to positive slope thereafter.

The $S(T)$ behavior depends on the competition among the various scattering mechanisms for the heat carriers and balances between the electron and phonon competition. It is worth emphasizing that $S(T)$ increases linearly above 70 K and is well reproduced from the present theoretical model; this phenomenon is attributed to the shortened phonon mean free path as compared to that at low temperatures. It may be seen that the slope change in $S_{\mathrm{ph}}^{\mathrm{drag}}$ is much more pronounced than that in $S_{\mathrm{c}}^{\mathrm{diff}}$ below 150 K. The reason for this change is due to the fact that the phonon-impurity scattering dominates and electron-impurity scattering is weaker. Below T_c, the opening of the superconducting gap rapidly reduces the phonon-electron scattering rate, and the competition in

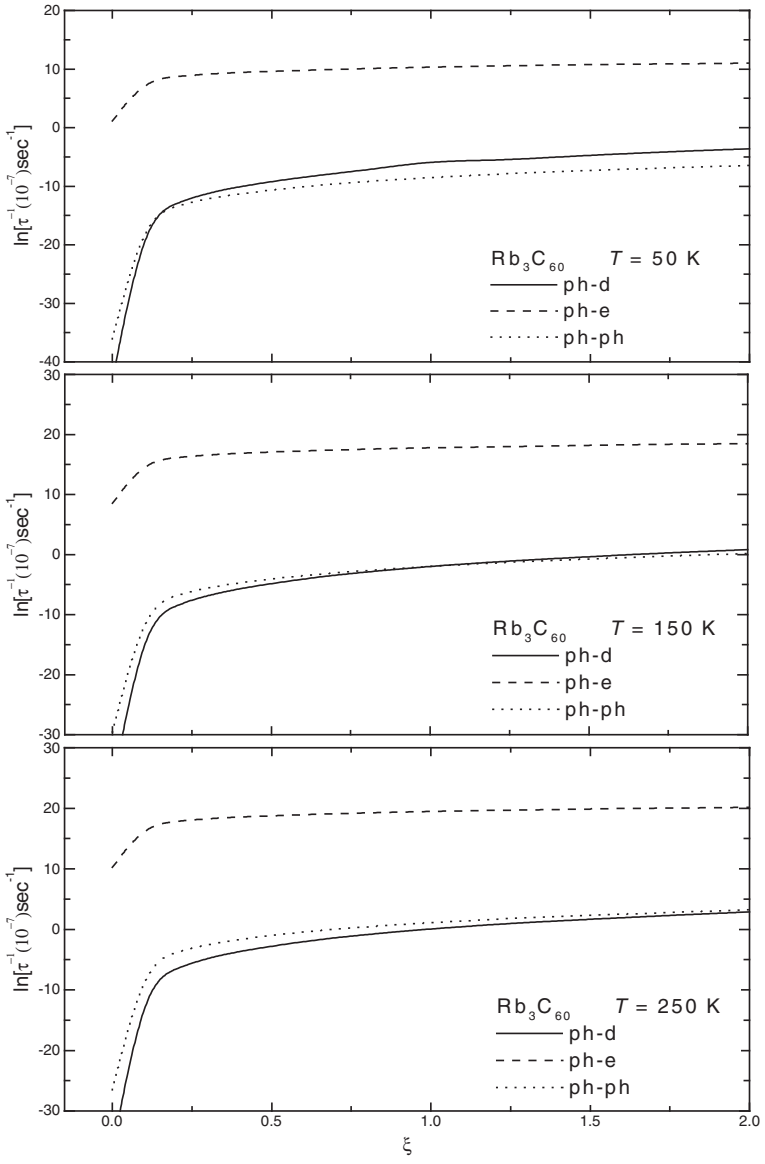

Figure 3 Variation of phonon relaxation times as function of ξ for T = 50, 150, and 250 K. For Rb_3C_{60} superconductors.

between phonon-impurity and phonon-electron scattering mechanism leads to faster change of slope in S_{ph}^{drag}.

The reason is further related to the fact that the mean free path of both electrons and phonons changes below T_c because the scattering of phonons on electrons is reduced when electrons condense in the superconducting state. Deduced results on temperature dependence of thermoelectric power of Rb_3C_{60} from the present model are consistent qualitatively with the experimental data [10,12]. Apart from the qualitative agreement at low temperature, the diffusive thermoelectric power improves on phonon-drag thermoelectric power at room temperature. The reason for this is the shorter mean free path of carriers in the normal state. However, below T_c, where the concentration of charge carrier is decreased by the formation of a Cooper pair and the phonon mean free path becomes longer, S_c^{diff} continues to play an important role even near room temperature.

It is customary to mention that a change in slope of S_{ph}^{drag} is obtained at about $T \approx \theta_D$, as in the normal metals [9]. Indeed, below $T \approx \theta_D$, the temperature dependence of the phonon-drag contribution is attributed to be a competitive process in which $S(T)$ decreases on lowering temperature and slightly improves on increasing temperature which is attributed to phonon-phonon scattering. To an extent, a comparison of the computed data, a consistent fit with the reported data, was obtained by choosing a reasonable set of parameters. It

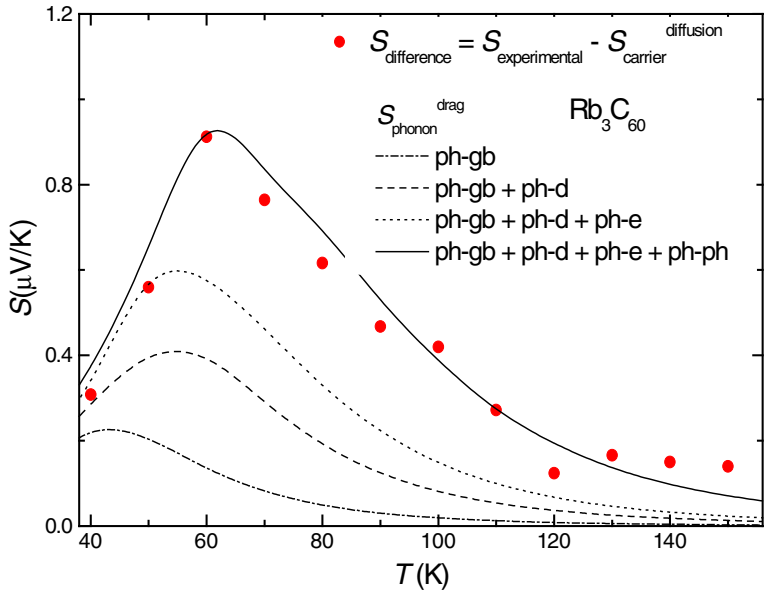

Figure 4 Variation of phonon-drag thermoelectric power as function of temperature in presence of various phonon scattering mechanism. A comparison is being made with the data obtained from Figure 1 as $S_{experimental} - S_c^{diff}$ for Rb_3C_{60} superconductors.

is instructive to compare the observation with that of conventional superconductors where the thermally excited quasiparticles of the electron system are dominant carriers of heat; a similar situation is revealed in Rb_3C_{60}.

Conclusions

The thermoelectric power $S(T)$ behavior is an instructive probe to reveal the lattice effects and carrier diffusion as well the interaction of these excitations with one another with impurities, grain boundaries, and defects. Among various transport probes, it brings information about available subsystems, and the measurements are fairly simple. The present study intends to contribute towards a thorough understanding of the scattering processes taking place in this fascinating material. The thermoelectric power behavior exhibits nearly T-linear dependence above T_c, a broad peak around 70 K, and further deviation from T-linear dependence above 200 K. In order to simulate the actual situation occurring in the temperature-dependent behavior of $S(T)$ in Rb_3C_{60}, we considered two channels to S (T): carrier diffusion or S_c^{diff} using the Mott expression within parabolic band approximation and phonon drag or S_{ph}^{drag}.

S_{ph}^{drag} is discussed within the Debye-type relaxation rate approximation in terms of acoustic phonon frequency, a relaxation time τ, and the sound velocity. The total phonon relaxation rate is the sum of terms corresponding to independent scattering mechanism, like defects, grain boundaries, and phonons and holes as carriers dominating in different temperature intervals. We have made a careful analysis taking into account several different processes that could exist in this material whose interaction can yield the observed dependence.

The quasiparticles caused an increase of the carrier heat and a slow increase of the phonon contribution below T_c. The rapid increase in $S(T)$ is attributed to the increase in phonon mean free path due to carrier condensation in the superconducting state limited by various impurity scattering mechanisms. The physical entities in the present scheme that characterize the strengths of the phonon-defect, phonon-electron, and phonon-phonon scattering lead to a result that successfully retrace the experimental curve.

The anomalous behavior around 70 K is attributed to electron-phonon interactions. The model calculations assume electrons as carriers using Mott expression within parabolic band approximation for thermoelectric power, and the negative behavior of S up to room temperature with a value of 18.9 μV/K is in good agreement with the room-temperature values in the range 10 to 20 μV/K. It is known that the satisfactory explanation of these peculiar properties is constrained as electron, and the lattice contributes to the thermoelectric power because both contributions are limited by various scattering mechanisms. Despite the limitations and use of material parameters for the estimation of transport coupling strengths, the present theoretical model on the thermoelectric power of the Rb_3C_{60} consistently reveals the interesting behavior reported experimentally. The intermolecular acoustic phonons are solely

responsible for the thermoelectric power behavior; however, electron-intramolecular phonon interaction is key for superconductivity.

Conclusively, thermoelectric power is one of those important transport entities which exhibit nonzero values in both the normal and superconducting state. Its behavior is determined by competition among the several operating scattering rates for the heat carriers and a balance between diffusive carrier, and phonon-drag contributions with acoustic phonons are effectively scattered by various scatterers for thermoelectric power. Moreover, the scatterings of quasiparticles are constrained by impurities as clearly evidenced in orientationally disordered Rb_3C_{60}. Despite the limitations, the present approach successfully describes the nearly T-linear dependence above T_c, a broad peak around 70 K, and further deviation from T-linear dependence above 200 K of thermoelectric power in Rb_3C_{60}. Although we have provided a simple phenomenological explanation of this effect, there is clearly a need for a good theoretical understanding of the transport.

Competing interests
The authors declare that they have no competing interests.

Authors' contributions
DV suggested and formulated the problem for investigation. NS is essentially involved in the computation of all physical parameters. All authors have equally participated in drawing conclusions, writing results, and completing the paper. All authors read and approved the final manuscript.

Authors' information
DV is a professor in the School of Physics, Devi Ahilya University, Indore, India. NS is an assistant professor in the Department of Physics, Ranchi College, Ranchi University Ranchi.

Acknowledgements
Namita Singh is thankful to Prof. SN Singh, PG Department of Physics, Ranchi University, Ranchi, Jharkhand and Dr. Khursheed Akhtar, Department of Chemistry, Ranchi College, Ranchi, Jharkhand, India for their useful discussions.

Author details
[1]Materials Science Laboratory, School of Physics, Vigyan Bhawan, Devi Ahilya University, Khandwa Road Campus, Indore 452001, India. [2]Department of Physics, Ranchi College, Ranchi University Ranchi, Jharkhand 834008, India.

Received: 19 June 2012 Accepted: 4 November 2012
Published: 28 November 2012

References
1. Hebard, AF, Rosseinsky, MJ, Haddon, RC, Murphy, DW, Glarum, SH, Palstra, TTM, Ramirez, AP, Kortan, AR: Superconductivity at 18 K in potassium-doped C_{60}. Nature **350**, 600 (1991)
2. Forro, L, Mihaly, L: Electronic properties of doped fullerenes. Rep. Prog. Phys. **64**, 649 (2001)
3. Gunnarson, O: Superconductivity in fullerides. Rev. Mod. Phys. **69**, 575 (1997)
4. Pekker, S, Janossy, A, Mihaly, L, Chauvet, O, Carrard, M, Forro, L: Single-crystalline $(KC_{60})_n$: a conducting linear alkali fulleride polymer. Science **265**, 1077 (1994)
5. Prassides, K, Tomkinson, J, Christides, C, Rosseinsky, MJ, Murphy, DW, Haddon, RC: Vibrational spectroscopy of superconducting K_3C_{60} by inelastic neutron scattering. Nature **354**, 462 (1991)
6. Tycko, R, Dabbagh, G, Rosseinsky, MJ, Murphy, DW, Ramirez, AP, Fleming, RM: Electronic properties of normal and superconducting alkali fullerides probed by ^{13}C nuclear magnetic resonance. Phys. Rev. Lett. **68**, 1912 (1992)
7. Chen, CT, Tjeng, LH, Rudolf, P, Meigs, G, Rowe, JE, Chen, J, McCauley, JP, Smith, AB, McGhie, AR, Romanow, WJ, Plummer, EW: Electronic states and phases of K_xC_{60} from photoemission and X-ray absorption spectroscopy. Nature (London) **352**, 603 (1991)
8. Rotter, LD, Schlesinger, Z, McCauley Jr, JP, Coustel, N, Fischer, JE, Smith III, AB: Infrared reflectivity measurements of a superconducting energy scale in Rb_3C_{60}. Nature **355**, 532 (1992)
9. Mott, NF, Davis, EA: Electronic processes in non-crystalline materials. Clarendon, Oxford (1979)
10. Inabe, T, Ogata, H, Maruyama, Y, Achiba, Y, Suzuki, S, Kikuchi, K, Ikemoto, I: Electronic structure of alkali metal doped C_{60} derived from thermoelectric power measurements. Phys. Rev. Lett. **69**, 3797 (1992)
11. Wang, ZH, Fung, AWP, Dresselhaus, G, Dresselhaus, MS, Wang, KA, Zhou, P, Eklund, PC: Electron–electron interactions and superconducting fluctuations in weakly localized K_3C_{60}. Phys Rev B **47**, 15354 (1993)
12. Sugihara, K, Inabe, T, Maruyama, Y, Achiba, Y: Thermoelectric power of alkali doped C_{60}. J Phys Soc Jpn **62**, 2757 (1993)
13. Morelli, DT: Thermoelectric power of superconducting fullerenes. Phys Rev B **49**, 655 (1994)
14. Kaiser, AB: Electron–phonon interaction and thermopower nonlinearities in Chevrel-phase compounds. Phys Rev B **35**, 4677 (1987)
15. Kaiser, AB, Uher, C: Thermoelectricity of high-temperature superconductors. In: Narlikar, A (ed.) Studies of High Temperature Superconductors, vol. 7, p. 353. Nova Science Publishers, New York (1991)
16. Uher, C: Thermal conductivity of high-temperature superconductors. In: Ginsberg, DM (ed.) Physical Properties of High Temperature Superconductors, vol. 3, p. 159. World Scientific, Singapore (1992)
17. Grivei, E, Cassart, M, Issi, JP, Langer, L, Nysten, B, Michenaud, JP, Fabre, C, Rassat, A: Anomalous specific heat of C_{60}. Phys Rev B **48**, 8514 (1993)
18. Varshney, D: Effect of impurity scatterers on phonon, electron and magnon thermal transport in electron doped cuprate superconductors Supercond. Part. Sci. Technol. **19**, 433 (2006)
19. Callaway, J: Quantum theory of the solid state. Academic Press, London (1991)
20. Barnard, RD: Thermoelectricity in metals and alloys. Taylor and Francis Ltd, London (1972)
21. Varshney, D, Tosi, MP: Pairing mechanism and superconducting state parameters of cubic perovskite $Ba_{0.6}K_{0.4}BiO_3$. J. Phys. Chem. Solids **61**, 683 (2000)
22. Ramirez, AP, Kortan, AR, Rosseinsky, MJ, Duclos, SJ, Mujsce, AM, Haddon, RC, Murphy, DW, Makhija, AV, Zahurak, SM, Lyons, KB: Isotope effect in superconducting Rb_3C_{60}. Phys. Rev. Lett. **68**, 1058 (1992)
23. Erwin, SC, Pickett, WE: Theoretical normal-state transport properties of K_3C_{60}. Phys Rev B **46**, 14257 (1992)

doi:10.1186/2251-7235-6-37
Cite this article as: Varshney and Singh: **Thermoelectric power of metallic Rb_3C_{60}: phonon-drag and carrier diffusion contributions.** *Journal of Theoretical and Applied Physics* 2012 **6**:37.